

Stable and Metastable Structures of Cobalt on Cu(001): An *ab initio* Study

R. Pentcheva and M. Scheffler

Fritz-Haber-Institut der Max-Planck-Gesellschaft, Faradayweg 4-6, D-14195 Berlin-Dahlem, Germany
(Received 12 August 1999)

We report results of density-functional theory calculations on the structural, magnetic, and electronic properties of (1×1) -structures of Co on Cu(001) for coverages up to two monolayers. In particular we discuss the tendency towards phase separation in Co islands and the possibility of segregation of Cu on top of the Co-film. A sandwich structure consisting of a bilayer Co-film covered by 1ML of Cu is found to be the lowest-energy configuration. We also discuss a bilayer $c(2 \times 2)$ -alloy which may form due to kinetic reasons, or be stabilized at strained surface regions. Furthermore, we study the influence of magnetism on the various structures and, e.g., find that Co adlayers induce a weak spin-density wave in the copper substrate.

8.35.-p, 68.55.-a, 71.20.Be

I. INTRODUCTION

Heteroepitaxial structures of Co and Cu exhibit intriguing magnetic properties such as giant magnetoresistance¹, interlayer exchange coupling², and surface magnetic anisotropy³. Since these properties are closely related to the surface and interface morphology, identification and understanding of the atomic structures and energetics of the adsorption of cobalt on the copper surface are of great interest. Specifically we discuss in this paper the [001]-surface orientation. Thin films deposited on a substrate of a different material are generally subject to strain arising from the different lattice parameters of the adsorbate and substrate. Our calculations show that the lattice constant of a ferromagnetic fcc bulk phase of Co is 2.8% smaller than that of a fcc Cu crystal, while the lattice constant of a hypothetical nonmagnetic fcc cobalt crystal is 4.3% smaller than that of the copper crystal. Here we take the fcc structure of cobalt, because it has been shown that a thick epitaxial cobalt film on Cu(001) can be characterized in terms of a tetragonally distorted face centered cubic (fct) phase⁴. The lattice mismatch between cobalt and copper suggests a small tensile strain. However for ultrathin films ($\Theta < 2$ ML) the comparison of the bulk phases of adsorbate and substrate is not necessarily very relevant. For example total-energy calculations⁵ show that the equilibrium lattice constant of an unsupported Co monolayer is 14.1% (nonmagnetic case) and 12.2% (ferromagnetic case) smaller than the Cu bulk lattice constant, implying that an ultrathin film might be subject to a much stronger tensile strain than a thick overlayer. The relation between lattice mismatch and relaxation of the interlayer spacing will be discussed in Section IV below.

While experimental studies of coverages above 2ML show that growth proceeds in an almost perfect layer-by-layer mode, for the initial two layers a deviation from the Frank-van der Merwe (FM) growth mode and a strong dependence on the growth conditions was reported⁶. Angle-resolved X-ray photoemission spectroscopy (ARXPS) data⁷ indicate that the second layer begins to form before the first layer is completed. As-

suming the coexistence of areas of clean Cu(001) surface and of monolayer and bilayer islands, a LEED analysis⁸ estimated that for a total coverage of one monolayer and deposition rates ranging between 0.016 and 0.33 ML/s the area covered by bilayer islands at room temperature is 20 – 40%. Fassbender *et al.*⁶ performed STM-experiments at room temperature for a total coverage of 1.35 ML and report that the fractional layer filling depends strongly on the deposition rate. For a low (0.003 ML/s) deposition rate they found that the first layer was closed and 0.35ML were in the second layer, while for a high deposition rate (0.3 ML/s) 15% of the surface was still uncovered and about 50% of the surface was already covered by bilayer high islands.

X-ray photoemission scattering (XPS)⁷, Auger electron scattering(AES) and STM measurements⁹ show an increase of the Cu signal and decrease of the Co signal upon annealing which was interpreted as segregation of substrate material on top of the cobalt layer. Similar results were reported for Fe/Cu(001)¹⁰. This effect was explained in terms of the lower surface energy of Cu compared to Co. We note that the application of this argument to thin film systems is not trivial because of the energy cost of the additionally created Cu/Co interface. Yet our studies show that in the case of Co on Cu(001) the contribution of the interface energy is very small (see Section III).

The impact of morphological changes on the magnetic properties of Co/Cu(001) was recently investigated with X-ray magnetic circular dichroism (XMCD) and magneto optical Kerr effect (MOKE)¹¹ experiments. At a cobalt coverage of 1.8 ML a sudden jump of the Curie temperature was measured which changed strongly with time or a subsequent heat treatment. The authors speculated that the critical thickness coincides with the thickness at which bilayer cobalt islands coalesce.

Depending on growth conditions (temperature, deposition rate), significantly different structures are observed experimentally. Although the magnetic properties of Co on Cu(001) have been the subject of many theoretical studies, a systematic theoretical analysis of the different configurations and their relative stability is still lacking.

Moreover most of the calculations^{13,14} have used slabs with atomic positions frozen to the bulk coordinates of the substrate, neglecting thus the structural relaxation of the clean Cu(001) surface and of the Co/Cu(001) adsorbate system.

In this paper we focus on the behavior of Co on Cu(001) under thermodynamic equilibrium conditions. We performed density-functional theory calculations considering a variety of configurations ($\theta \leq 2$ ML). In particular we discuss two aspects: the formation of multilayer cobalt islands and sandwich structures with a copper capping. For each system we performed a full structure optimization and establish the relation between the energetic trends and the structural, magnetic and electronic properties. The paper is organized as follows: The details of the calculations are given in Section II. In Section III we discuss the stability of the systems against separation in multilayer islands and the influence of the capping layer. The structural (Section IV), magnetic (Section V) and electronic (Section VI) properties of mono- and bilayer cobalt films on Cu(001), as well as of the corresponding copper capped systems are investigated. Finally in Section VII we address the similarities and differences between Co/Cu(001) and Co/Cu(111) referring to STM and *ab initio* results for the [111]-orientation¹⁵. The results are summarized in Section VIII.

II. CALCULATIONAL DETAILS

Our calculations are performed using density-functional theory (DFT). The exchange-correlation functional is treated within the local-density approximation (LDA)¹⁶ and for the magnetic systems we performed spin-polarized calculations within the local spin-density approximation (LSDA). We also examined the possible importance of non-local exchange correlation effects by employing the generalized-gradient approximation (GGA) in the parameterization of Perdew, Burke, and Ernzerhof¹⁷. The results show that for our study LDA and GGA give the same structural and energetic trends. More details on this issue will be discussed in the Appendix.

The Kohn-Sham equation was solved applying the full-potential linearized augmented plane wave (FP-LAPW) method^{18,19}. The surface is simulated by repeated slabs separated in z -direction by a vacuum region. Co is adsorbed on both sides of the substrate. The thickness of the vacuum region between the slabs, corresponding to 6 Cu layers (10.65 Å), is found to be sufficient to avoid interactions of the Co atoms. The interlayer distances d_{12} and d_{23} were optimized with a damped Newton dynamics and the relaxations $\Delta d_{12}/d_0$ and $\Delta d_{23}/d_0$ are given with respect to the interlayer spacing of a Cu crystal, d_0 . Referring the Co-Cu and for Co bilayer systems even the Co-Co interlayer distances to the interlayer spacing of Cu is probably not an optimum choice, but it is well defined

$N_{\mathbf{k}_{\parallel}}$	E_{cut} [Ry]	E^{f} [eV/(1 × 1)-cell]	ϕ [eV]
6	15.6	1.50	5.27
15	15.6	1.51	5.29
21	15.6	1.51	5.29
28	15.6	1.51	5.28
36	15.6	1.51	5.28
45	15.6	1.51	5.28
21	12.8	1.58	5.31
21	13.8	1.53	5.29
21	17.5	1.50	5.27

TABLE I. Convergence tests performed within LDA for a 5-layer slab of Co(001) strained at the lattice constant of copper and interlayer distance optimized for $N_{\mathbf{k}_{\parallel}} = 28$. The surface energy E^{f} and work function ϕ are given as a function of the plane wave cut-off E_{cut} and the number of \mathbf{k}_{\parallel} -points in the irreducible part of the Brillouin zone $N_{\mathbf{k}_{\parallel}}$.

and has been the common practice for such adsorbate systems. We therefore use this convention here as well.

The lattice constant for the fcc copper crystal $a_{\text{Cu}} = 3.55$ Å, obtained from a non-relativistic calculation, is 1.6% smaller than the measured one (3.61 Å), 0.1% of which reflects our neglect of zero point vibrations in the theory. The lateral lattice parameter of the Cu substrate was set to the calculated lattice constant for a fcc copper crystal. We chose a muffin tin (MT) radius of $R_{\text{Cu}}^{\text{MT}} = 2.20$ bohr for the Cu atoms and a slightly smaller radius $R_{\text{Co}}^{\text{MT}} = 2.15$ bohr for the Co atoms to prevent overlap of the MT spheres due to the strong relaxation found for some systems.

The stability of various systems is analyzed with respect to the formation energy. Assuming that the slab is in thermal equilibrium with a Co and a Cu crystal, acting as reservoirs of Co and Cu atoms, the formation energy in eV per (1 × 1)-unit cell is defined as:

$$E^{\text{f}} = \frac{1}{2A} (E^{\text{slab}} - N_{\text{Cu}} E_{\text{Cu}}^{\text{bulk}} - N_{\text{Co}} E_{\text{Co}}^{\text{bulk}}), \quad (1)$$

where A is the area of the surface unit cell of the considered slab²¹ and the factor 2 accounts for the presence of two surfaces of the slab. N_{Cu} and N_{Co} are the number of Cu and Co atoms in the slab supercell and $E_{\text{Cu}}^{\text{bulk}}$ and $E_{\text{Co}}^{\text{bulk}}$ are the energies of a Cu or a Co atom in the respective fcc bulk crystals at the theoretical equilibrium lattice constants. Thus for a pure Cu slab ($N_{\text{Co}} = 0$) E^{f} is the Cu surface energy, and for a pure cobalt slab ($N_{\text{Cu}} = 0$) with $a_{\parallel} = a_{\text{Co}}$ it is the surface energy of cobalt.

The LAPW wave functions within the muffin tins (MTs) were expanded in spherical-harmonics with angular momenta up to $l_{\text{max}}^{\text{wf}} = 10$. Non-spherical contributions to the electron density and potential within the MTs were considered up to $l_{\text{max}}^{\text{pot}} = 4$. The cutoff for the Fourier-series expansion of the interstitial electron density and potential was chosen to be $G_{\text{max}} = 12.0$ bohr⁻¹. Extensive convergence tests with respect to \mathbf{k}_{\parallel} -point set and the energy cutoff for the basis set were performed

N_{layer}	E^{f} [eV/(1 × 1)-cell]	ϕ [eV]	$\Delta d_{12}/d_0$ [%]
3	0.79	4.91	-2.93
5	0.78	4.78	-3.01
7	0.78	4.83	-3.10
9	0.78	4.82	-3.11

TABLE II. DFT-LDA results for the surface energy E^{f} , work functions ϕ , and relaxation $\Delta d_{12}/d_0$ of the clean Cu(001)-surface are given as a function of the number of slab layers N_{layer} , $N_{\mathbf{k}} = 21$, $E_{\text{cut}} = 15.0$ [Ry].

N_{layer}	E^{f} [eV/(1 × 1)-cell]	ϕ [eV]
3	1.767	5.31
5	1.754	5.31
7	1.753	5.30
9	1.759	5.30

TABLE III. Formation energy and work functions for 1Co/Cu(001) with optimized interlayer distances as a function of the number of substrate layers N_{layer} .

for a 5-layer Co(001) slab at the lattice constant of copper and relaxed interlayer distance. The results are shown in Table I. A numerical accuracy of 6% for the formation energy is achieved with $E_{\text{cut}} = 12.8$ Ry, while $E_{\text{cut}} = 15.6$ Ry is needed for an accuracy of 1%. Thus a cutoff parameter of 15.6 Ry was chosen throughout the calculations. The Brillouin-zone integration was performed with a special point set generated after the scheme of Monkhorst and Pack²². We obtained an accuracy of the Brillouin-zone integration better than 1% by using 21 \mathbf{k}_{\parallel} -points in the irreducible wedge of the Brillouin-zone (IBZ) (see Table I).

The bulk energies needed as a reference to determine the formation energy (see Eq.(1)) were calculated using the same LAPW-parameters as in the slab calculations. For the bulk calculation 104 \mathbf{k} -points in the IBZ were used.

Prior to investigating the effects of adsorption of cobalt, we checked the required thickness of a copper slab, to ensure a good representation of the properties of the clean Cu(001)-surface. The surface energies, work functions and interlayer relaxations for slabs of 3, 5, 7, and 9 layers of copper are compared in Table II. For a 5-layer slab the relaxation between surface and subsurface layer of -3.01% is close to the experimental value obtained by MEIS²³ (-2.4%) while the LEED-result²⁴ is smaller ($-1.1 \pm 0.4\%$). The calculated work function $\phi = 4.78$ eV is in good agreement with experiment: 4.59 ± 0.05 eV²⁵, 4.76 eV²⁶, and 4.77 ± 0.05 eV²⁷.

A further requirement of the thickness of the slab is that the interaction of the Co layers on both sides of the slab through the substrate is negligible for the questions of concern. To test the strength of this interaction we studied the formation energy and work function for 1ML Co on Cu(001) (1Co/Cu(001)) as a function of the substrate thickness. The results are summarized in Table

System	E^{f} [eV/(1 × 1)-cell]	ϕ [eV]
Cu(001)	0.78	4.78
1Co/Cu(001) NM	1.75	5.31
1Co/Cu(001) FM	1.51	5.16
2Co/Cu(001) NM	1.55	5.38
2Co/Cu(001) FM	1.42	4.88
1Cu/1Co/Cu(001) NM	1.27	4.89
1Cu/1Co/Cu(001) FM	1.18	4.81
1Cu/2Co/Cu(001) NM	1.14	4.74
1Cu/2Co/Cu(001) FM	1.12	4.82
bilayer Co-Cu-c(2 × 2)-alloy NM	1.48	5.18
bilayer Co-Cu-c(2 × 2)-alloy FM	1.36	4.97

TABLE IV. Formation energies E^{f} and the work functions ϕ for various structures.

III. Both the formation energy and work function converge quickly with the substrate thickness. On the basis of these results we conclude that a 5-layer copper slab represents a good approximation of the Cu(001)-surface.

III. FORMATION ENERGY AND STABILITY

In order to identify the equilibrium configuration of Co on Cu(001) we investigate in this Section the tendency towards separation in multilayer islands and the influence of a copper capping layer. The studied systems include the clean Cu(001) surface, a monolayer and bilayer thick cobalt film on Cu(001) denoted by 1Co/Cu(001) and 2Co/Cu(001), respectively, as well as the corresponding capped systems, 1Cu/1Co/Cu(001) and 1Cu/2Co/Cu(001). Additionally we investigated a bilayer Co-Cu-c(2 × 2)-alloy. The calculated formation energies and the work functions are given in Table IV. We consider several ways in which a total coverage of 1ML Co can be arranged on a Cu(001) surface. The energy of a system consisting of more than one domain, namely regions of clean copper surface and regions covered by large cobalt islands, is simply given by the weighted sum of the formation energy of the clean Cu(001) surface and those of the Co-island. Under the assumption that the islands are large, the contributions of the step edges and side facets of the islands are negligible and were not taken into account. A schematic presentation of the different structures are given in Fig. 1 together with energy changes with respect to the case where the whole surface is covered by a monolayer thick (1 × 1)-cobalt layer.

Our calculations show that a monolayer film, Fig. 1(a), would separate into a clean Cu(001)-surface and a bilayer island, Fig. 1(b). For the nonmagnetic case the gain in energy is $\Delta E^{\text{NM}} = 0.59$ eV/(1 × 1)-cell and for the ferromagnetic case it is $\Delta E^{\text{FM}} = 0.41$ eV/(1 × 1)-cell. This result can be explained in terms of the higher coordination of the cobalt atoms in the bilayer film and correlates with the substantial broadening of the cobalt d -band and the strong relaxation between Co layers in 2Co/Cu(001)

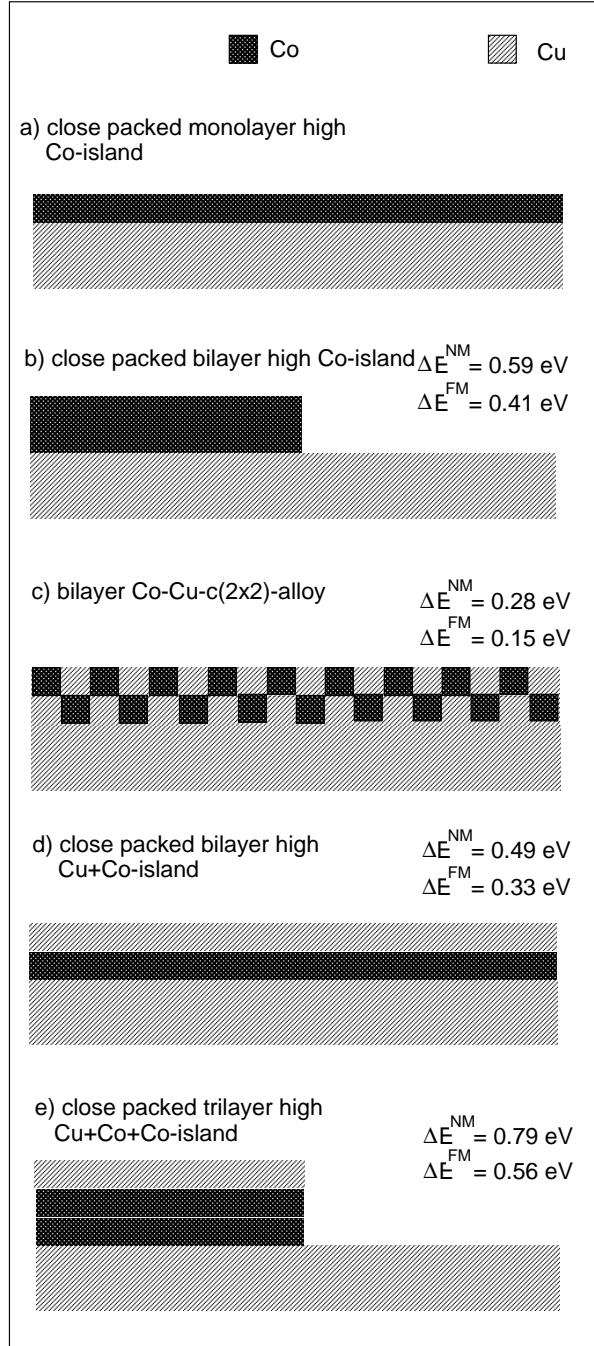


FIG. 1. Schematic diagram of the different adsorbate configurations for a Co coverage of $\Theta = 1.0$ ML. The formation energy changes for configurations b)-e) in the nonmagnetic ΔE^{NM} and ferromagnetic case ΔE^{FM} is given with respect to formation energy of the close packed monolayer high island shown in a).

as will be discussed later in this paper. Concerning the effect of magnetism, we see that it reduces, but does not change the tendency towards formation of bilayer islands.

Experimental studies^{7,9} show that copper segregates onto the surface after annealing. Therefore we study here the influence of a copper capping layer on stability. Covering $1\text{Co}/\text{Cu}(001)$ with a monolayer of copper, Fig. 1(d), reduces the energy of the system by $\Delta E^{\text{NM}} = 0.49$ eV/ (1×1) -cell. Compared to the cobalt terminated systems the copper-capped systems gain less spin-polarization energy because of the hybridization with the capping layer. Consequently the energy gain due to a capping layer for the magnetically ordered system is lower than the one for the nonmagnetic: ($\Delta E^{\text{FM}} = 0.33$ eV/ (1×1) -cell). The influence of the capping layer on the magnetic properties of the copper covered systems will be discussed in Section V. Saúl and Weissmann²⁸ recently calculated the surface segregation energy of $3d$ -impurities (Fe, Co, Ni) in Pd, Ag, and Cu. They found, in agreement with our results, that embedding in the bulk of the host material is connected with a substantial gain in energy both for nonmagnetic and magnetic impurities/(layers), the effect being weaker for the latter. We also note that the copper capping layer in the $1\text{Cu}/1\text{Co}/\text{Cu}(001)$ and $1\text{Cu}/2\text{Co}/\text{Cu}(001)$ systems has properties similar to the clean $\text{Cu}(001)$ -surface; for example we find that the work functions of the systems are $\phi_{\text{Cu}(001)} = 4.78$ eV, $\phi_{1\text{Cu}/1\text{Co}/\text{Cu}(001)} = 4.89$ eV, and $\phi_{1\text{Cu}/2\text{Co}/\text{Cu}(001)} = 4.74$ eV.

Recent combined STM and RHEED experiments²⁹ detected ordered $c(2 \times 2)$ regions when a total coverage of 1ML Co was deposited on $\text{Cu}(001)$ at room temperature and subsequently annealed at 450 K. Motivated by these results, we studied a configuration, where starting from $1\text{Co}/\text{Cu}(001)$ every other Co atom is replaced by a Cu atom in the substrate layer underneath. In this way a bilayer $c(2 \times 2)$ -alloy³⁰, shown schematically in Fig. 1(c), is formed. We find that this configuration is by 0.28 eV/ (1×1) -cell (nonmagnetic) and 0.15 eV/ (1×1) -cell (ferromagnetic case) more favorable than the (1×1) -monolayer in Fig. 1(a). However, it is a metastable structure because transition into a cobalt monolayer covered by copper, $1\text{Cu}/1\text{Co}/\text{Cu}(001)$ in Fig. 1(d), leads to an energy gain of 0.22 [eV/ (1×1) -cell] (nonmagnetic) and 0.18 eV/ (1×1) -cell (ferromagnetic case). Thus, the bilayer $c(2 \times 2)$ -alloy lies energetically between the $1\text{Co}/\text{Cu}(001)$ and $1\text{Cu}/1\text{Co}/\text{Cu}(001)$ systems and it may be stabilized kinetically. This surface alloy might also represent a favorable configuration with respect to surface strain relief. Indeed a $c(2 \times 2)$ -pattern was observed experimentally preferentially in the middle of large islands³¹.

We also studied whether the cobalt (1×1) -layer will prefer to be buried deeper in the substrate. Our calculations for the $1\text{Cu}/1\text{Co}/\text{Cu}(001)$ and $2\text{Cu}/1\text{Co}/\text{Cu}(001)$ systems show that there is no additional energy gain through covering the system with a thicker copper layer.

System	E_{NM}^{I}	E_{FM}^{I}
...Cu/1Co/Cu...	0.163	0.113
...Cu/2Co/Cu...	0.044	0.066
...Cu/3Co/Cu...	-0.005	0.046

TABLE V. Interface energies given in [eV/(1 × 1)-cell] for nonmagnetic (E_{NM}^{I}) and ferromagnetic (E_{FM}^{I}) systems as a function of the cobalt interlayer thickness.

The segregation of Cu on the surface is typically explained by the lower surface energy of Cu(001) compared to Co(001). Still this argument is only applicable if the interface energy were small and thus negligible. In order to calculate the energy cost to create an interface we studied three different systems with one, two and three cobalt interlayers in copper bulk, marked as (...Cu/1Co/Cu...), (...Cu/2Co/Cu...) and (...Cu/3Co/Cu...), respectively. Here the lateral parameter is set to the copper bulk value while the interlayer distances are relaxed. The interface energies, E^{I} , are calculated analogously to the formation energies [compare Eq.(1)]. In order to subtract the effect of elastic strain due to the lattice mismatch of the two materials we use as a reference energy for cobalt the bulk energy of fct cobalt with $a_{\parallel} = a_{\text{Cu}}$ and relaxed a_z ³² instead of the one of fcc cobalt at the cobalt lattice constant. Table V lists the results for nonmagnetic and ferromagnetic cobalt interlayers. It shows that the values of E^{I} for a cobalt bilayer and trilayer are very close, i.e. the interface energy converges quickly with the thickness of the cobalt layer. The interface energy is indeed significantly smaller than the difference of the surface energies of the clean Cu(001)-surface ($E^{\text{f}} = 0.79$ eV/(1 × 1)-cell) and a thick Co(001) film with a lateral parameter fixed to the lattice constant of copper and relaxed interlayer distances ($E_{\text{NM}}^{\text{f}} = 1.21$ eV/(1 × 1)-cell³³ and $E_{\text{FM}}^{\text{f}} = 1.11$ eV/(1 × 1)-cell³³). For this reason the common argument that simply the surface energy difference of cobalt and copper explains the segregation of substrate material on the surface works in the case of Co on Cu(001).

In analogy to the Co terminated system, the single Co layer capped by Cu shown in Fig. 1(d) will tend to separate into a clean Cu(001) surface and a double Co layer capped by Cu, Fig. 1(e). Still the energy gain due to phase separation [$\Delta E^{\text{NM}} = 0.31$ eV/(1 × 1)-cell, $\Delta E^{\text{FM}} = 0.23$ eV/(1 × 1)-cell] is only about half the energy gain for the system with Co on the surface. We can summarize that both the magnetic ordering and the capping layer weaken the tendency towards cobalt clustering but *qualitatively* we observe the same behavior with and without magnetism.

Yet we need to find out whether the bilayer film will be stable or if higher cobalt islands may form. In order to determine the formation energy of a N -layer ($N > 2$) thick cobalt island we assume that each of the *intermediate* cobalt layers has an energy of a bulk atom in a

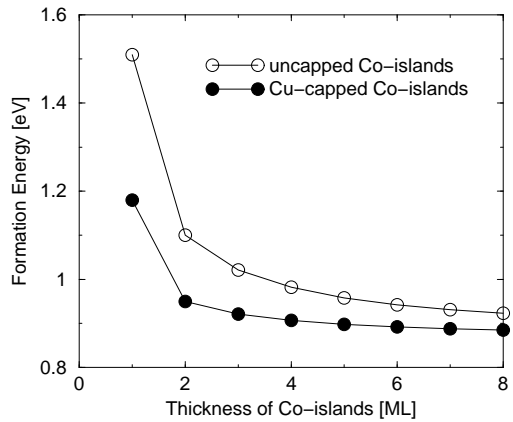


FIG. 2. Formation energy of different ferromagnetically ordered configurations for a total cobalt coverage of 1 ML as a function of the cobalt island thickness N . The structures consist of clean Cu(001) and a compact island with N Co layers (○) or N Co-layers capped by copper. The area covered by the cobalt islands is $\frac{1}{N}$ of the whole surface. Especially for the copper terminated systems the separation in higher than bilayer cobalt islands is unlikely because of a negligible energy gain.

tetragonal cobalt crystal with $a_{\parallel} = a_{\text{Cu}}$ and fully relaxed a_z ³². The elastic energy contribution is the difference between the energy of cobalt bulk at the fcc cobalt lattice constant and the energy of fct cobalt as described above and amounts to 0.11 eV (NM) and 0.08 eV (FM) per cobalt atom. Thus the formation energy of a N -layer cobalt film is

$$E_{N\text{Co}/\text{Cu}(001)}^{\text{f}} = E_{2\text{Co}/\text{Cu}(001)}^{\text{f}} + (N - 2)E^{\text{elast.}}. \quad (2)$$

For a total coverage of 1ML the formation energy of a configuration consisting of clean Cu(001) surface and a N -layers high cobalt island is given by:

$$E_{N\text{Co-island}}^{\text{f}} = \frac{1}{N}E_{N\text{Co}/\text{Cu}(001)}^{\text{f}} + \frac{N-1}{N}E_{\text{Cu}(001)}^{\text{f}}. \quad (3)$$

An analogous expression for the formation energy holds for the copper capped systems. The formation energy of the ferromagnetically ordered capped and uncapped systems is plotted in Fig. 2 as a function of cobalt-island height N . In the following we will concentrate on the Cu-terminated systems because, as can be seen from Fig. 2, they are always lower in energy. The substantial energy gain due to separation of a monolayer-thick cobalt film in bilayer islands was already discussed above. Yet further separation in higher cobalt islands brings only a small energy gain, e.g., the gain due to separation from bilayer in trilayer islands for the Cu-terminated islands is about 0.03 eV/(1 × 1)-cell. We note that this energy gain is mainly due to the increase of the clean Cu(001)-surface. Moreover the cost of the island facets, which was not taken into account in the present discussion, grows with island height. Because of the small energy gain, as shown

Method	$\Delta d_{12}/d_0$ [%]	$\Delta d_{23}/d_0$ [%]
1ML Co/Cu(001)		
FP-LAPW NM	-4.7%	-0.3%
FP-LAPW FM	-3.0%	0.0%
LEED ³⁶	-6.0%	-6.0%
LEED ⁸	-2.5%	-1.4%
2ML Co/Cu(001)		
FP-LAPW NM	-17.0%	0.0%
FP-LAPW FM	-13.4%	-0.8%
LEED ⁸	-2.0%	-4.2%
1ML Cu/1ML Co/Cu(001)		
FP-LAPW NM	-7.0%	-3.0%
FP-LAPW FM	-5.6%	-2.0%
1ML Cu/2ML Co/Cu(001)		
FP-LAPW NM	-5.0%	-14.8%
FP-LAPW FM	-4.6%	-12.5%

TABLE VI. Relaxation $\Delta d_{12}/d_0$ and $\Delta d_{23}/d_0$ of the interlayer spacing in % for the first two layers compared to the lattice parameter of Cu bulk, d_0 .

in Fig. 2, and the increasing cost of the sidewalls the formation of islands higher than bilayer is unlikely. We conclude that the ferromagnetically ordered configuration in Fig. 1(e), which is by 0.56 eV/(1 × 1)-cell more favorable than the one in Fig. 1(a), represents the thermodynamic equilibrium structure.

IV. STRUCTURAL PROPERTIES

In the previous Section we identified the bilayer cobalt island covered by a copper capping layer as the thermodynamically stable structure. However, crystal growth represents a situation which is more or less far from thermodynamic equilibrium therefore not only the equilibrium structure but also other, metastable, structures (e.g. those shown in Fig. 1) may occur. In this Section we present the results of a geometry optimization for monolayer and bilayer (1 × 1)- as well as copper-capped systems. The Co films are assumed to grow pseudomorphically on the Cu(001)-surface, adopting the lateral spacing of the Cu crystal. The calculated relaxation of the interlayer spacing for the nonmagnetic and ferromagnetic systems is given in Table VI. We remind the reader that all relaxations are given with respect to the interlayer spacing in copper bulk.

The first interlayer spacing in the monolayer film, $d_{\text{Co-Cu}}$, shows an inward relaxation of 4.7% for the nonmagnetic case, which reduces to 3.0% for the ferromagnetic film. At the same time the interlayer spacing between the first and second substrate layer, which is contracted by 3.0% for the clean Cu(001) surface, expands back to the bulk value -0.3% (0.0%) for the nonmagnetic (ferromagnetic) system. This result can be explained in terms of the bond-cutting model. Due to the miss-

ing bonds of the surface atoms the strength of the remaining bonds to the subsurface layer is enhanced, giving rise to an inward relaxation⁴⁰. The bond strength is also related to the d -band occupation⁴⁰, thus Co-Cu bonds are stronger than Cu-Cu bonds and consequently upon cobalt adsorption we observe a stronger relaxation of the Co-Cu-interlayer distance, while the Cu-Cu distance expands. Previous *ab initio* results¹² found a relaxation of the first interlayer distance of the ferromagnetic 1Co/Cu(001) surface of -10.4%. The reason for the discrepancy with our result (which is -3.0%) is in the choice of the lateral lattice parameter. While we use a non-relativistic treatment of the valence electrons and the corresponding theoretical equilibrium lattice constant of Cu (3.55 Å), Wu and Freeman¹² used a semi-relativistic treatment which gives a noticeably smaller lattice constant (3.52 Å). Nevertheless, in their adsorbate study Wu and Freeman¹² set the lateral lattice parameter to the substantially larger experimental value (3.61 Å). As a consequence, the strong interlayer relaxation found by Wu and Freeman¹² just reflects that their copper surface is under tensile strain. We tested this and indeed could reproduce the effect: When we use a semi-relativistic treatment of the valence electrons and still force the Cu substrate to assume the experimental lattice constant we obtain $\Delta d_{12}/d_0 = -7.9\%$ and $\Delta d_{23}/d_0 = -2.3\%$.

For the bilayer Co film we obtain a surprisingly strong contraction of the interlayer distance of $d_{\text{Co-Co}}$ of -17% in the nonmagnetic case. For the ferromagnetically ordered system the contraction is somewhat smaller, -13.4%, due to the magnetovolume effect. These results can hardly be explained by comparing the lattice constant of the fcc bulk phase of Co with that of bulk Cu. Such comparison would give a lattice mismatch of -4.3% in the nonmagnetic and -2.8% in the ferromagnetic case. Thus, in such description one would say that the Co film is strained, but that the effect is not very large. However, it is questionable whether the comparison of the bulk lattice parameters of the two materials, is a good approach for understanding ultrathin films with $\Theta \leq 2$ ML. For example, total-energy calculations based on the FP-LAPW method⁵ show that the difference between the equilibrium lattice constant of a *free standing* cobalt monolayer and that of the Cu substrate is -14.1% for a nonmagnetic and -12.2% for a ferromagnetic monolayer³⁵. Therefore, if we refer the strain in the Co adlayers to the lattice parameter of the free-standing Co layer, the strain is significant, and the above noted interlayer relaxation then simply reflects the reaction of the Co film to this big strain. Indeed, we think that this description is appropriate (in a qualitative sense) because for a very thin cobalt film ($\Theta \leq 2$ ML) the bonding to the noble metal substrate can only partially replace the bonds to missing cobalt neighbors. Thus, the adsorbed film will still bear some resemblance to the free-standing one. The above result also indicates that the weaker binding to the substrate is balanced by forming a strong bond between the two cobalt layers.

The competition between Co-Co and Co-Cu-bonding is also a driving force for the structural changes in the capped systems. The hybridization with the copper capping layer has the general effect of weakening the existing Co-Cu and Co-Co bonds in the 1Co/Cu(001) and the 2Co/Cu(001) system, respectively. Consequently, the interlayer distance between the cobalt and copper layer increases from -4.7% (NM) and -3.0% (FM) in 1Co/Cu(001) to -3.0% (NM) and -2.0% (FM) in 1Cu/1Co/Cu(001). Similarly the strong relaxation between the two cobalt layers decreases from -17.0% (NM) and -13.4% (FM) in 2Co/Cu(001) to -14.8% (NM) and -12.5% (FM) in 1Cu/2Co/Cu(001). On the other hand the stronger Co-Co bond induces a weaker binding with the capping layer which is reflected in the smaller inward relaxation of the distance between the capping layer and the cobalt film of -5.0% for the 1Cu/2Co/Cu(001) system compared to -7.0% for the 1Cu/1Co/Cu(001) system.

Table VI also contains structural data determined with LEED. We note, however, that such structural analysis is complicated and not unambiguous, because, as discussed above, in the Co/Cu(001) system several domains and/or metastable structures may coexist. In the absence of knowledge about these various structures and their energies, it appeared to be a reasonable choice for Clarke *et al.*³⁶ to assume that Co on Cu(001) will form a full Co monolayer. And based on this assumption they determined an inward relaxation of -6% for both $d_{\text{Co-Cu}}$ and $d_{\text{Cu-Cu}}$. Our work, however, shows that the 1Co/Cu(001) system is unstable with respect to the formation of bilayer islands and capped bilayers structures. In a more recent LEED study Cerda *et al.*⁸ assumed the coexistence of regions of clean Cu(001), Co monolayer and Co bilayer islands, but Co layers with a Cu capping layer, which we find to have the lowest total energy, were not considered. Thus, in both experimental analyses the model assumptions didn't include all relevant systems.

V. MAGNETIC PROPERTIES

The layer-resolved magnetic moments in the four systems studied, 1Co/Cu(001), 2Co/Cu(001), 1Cu/1Co/Cu(001) and 1Cu/2Co/Cu(001) are given in Table VII. To be precise, these are the contributions from the muffin tin region only. The top layer in 1Co/Cu(001) exhibits an enhanced magnetic moment ($M_{\text{Co(S)}} = 1.71 \mu_B$) compared to the bulk value of $1.52 \mu_B$, calculated at the equilibrium lattice constant of cobalt. This is due to the larger lateral constant of the epitaxial cobalt adlayer and to the reduced coordination on the surface. Further we find that the surface layer of the 2Co/Cu(001) system exhibits the same magnetic moment ($1.71 \mu_B$) as the 1Co/Cu(001) system. In fact, a thick fcc cobalt film at the lattice constant of copper also has a similar moment, namely $1.78 \mu_B$. However,

System	layer	$M [\mu_B]$
1Co/Cu(001)	Cu(C)	-0.004
	Cu(S-2)	-0.014
	Cu(S-1)	0.024
	Co(S)	1.711
2Co/Cu(001)	Cu(C)	-0.002
	Cu(S-3)	-0.009
	Cu(S-2)	0.016
	Co(S-1)	1.472
Co(001) at a_{Cu}	Co(C)	1.648
	Co(S-1)	1.615
	Co(S)	1.783
1Cu/1Co/Cu(001)	Cu(C)	-0.001
	Cu(S-3)	-0.008
	Cu(S-2)	0.027
	Co(S-1)	1.445
1Cu/2Co/Cu(001)	Cu(S)	0.040
	Cu(C)	-0.001
	Cu(S-4)	-0.007
	Cu(S-3)	0.022
1Cu/2Co/Cu(001)	Co(S-2)	1.383
	Co(S-1)	1.374
	Cu(S)	0.035

TABLE VII. Layer resolved local magnetic moments in the ferromagnetic systems in $[\mu_B]$ as obtained from the slab calculation. S, S-1, S-2, etc. denote the position of the corresponding layer with respect to the surface, S being the surface layer and C being the central layer of the slab.

the magnetic moment of the subsurface Co layer, which binds to the Cu substrate, is reduced to $1.47 \mu_B$. The corresponding magnetic moment of subsurface cobalt in a thick fcc cobalt film at the lattice constant of copper is $1.62 \mu_B$. The lower magnetic moment of subsurface cobalt is a consequence of the higher coordination and the strong contraction of the interlayer spacing $d_{\text{Co-Co}}$.

The hybridization with the copper capping layer reduces the magnetic moment of the first Co layer both in the 1Cu/1Co/Cu(001) and 1Cu/2Co/Cu(001) systems by about $0.3 \mu_B$ compared to the 1Co/Cu(001) and 2Co/Cu(001) systems. It is interesting to note that both Co layers in 1Cu/2Co/Cu(001) have the same magnetic moment ($1.38 \mu_B$) which can be explained by the fact that Co(S-1) and Co(S-2) have the same coordination of Co and Cu atoms.

To our knowledge magnetic moments for 1Co/Cu(001) have not yet been measured due to the already discussed difficulties in the preparation of a single cobalt monolayer on Cu(001). Our calculated value of the surface magnetic moment of 1Co/Cu(001), $1.71 \mu_B$, is slightly lower than that obtained in previous calculations, e.g. $1.78 \mu_B$ ¹² and $1.76 \mu_B$ ¹³ from FP-LAPW and $1.85 \mu_B$ ¹⁴ from FP-LMTO (full-potential linearized muffin tin orbitals) calculations. The differences are attributed mainly to the use of the experimental lattice constant of copper (3.61 \AA) and/or the lack of consider-

ing the interlayer relaxation in Refs.^{12–14} (see also Section IV).

The magnetic moments of 1.9 ML and 2.1 ML of Co deposited on Cu(001) measured with x-ray magnetic circular dichroism (XMCD) are $1.71 \pm 0.1 \mu_B$ ³⁷ and $1.77 \pm 0.1 \mu_B$ ³⁸, respectively. The XMCD-spectra were recorded at 40 K, but information about the preparation conditions, which could tell whether the Co layers were capped by Cu, is not available. Yet, the magnetic moment compares well with our calculated magnetic moment for 2Co/Cu(001). With respect to other theoretical work, we note that the same trend of an enhanced magnetic moment in the surface layer ($1.85 \mu_B$) and a reduced magnetic moment in the subsurface layer ($1.60 \mu_B$) was found in a previous FP-LAPW calculation for 2Co/Cu(001)³⁹. In this study the lateral parameter was fixed to the experimental lattice constant of copper and relaxation of the interlayer spacing was not taken into account. However, the strong relaxation of the interlayer spacing in 2Co/Cu(001) discussed in Section IV has a noticeable influence on the magnetic moments and cannot be neglected.

Our results reveal also that the adsorbed cobalt film induces a small polarization in the substrate. The magnetic moment of the copper layer at the interface is positive, e.g. in 1Co/Cu(001) it is $0.024 \mu_B$. Then, in the next layer it switches to a negative value ($-0.014 \mu_B$). Also the central layer of our 5-layer Cu slab has a very small negative moment, $-0.004 \mu_B$. The oscillation of the magnetic moment perpendicular to the surface indicates the formation of a spin-density wave. This striking effect is observed for all four studied systems. However, we note that for a detailed investigation of this effect, a thicker substrate slab has to be considered. The magnetic moment induced in the capping layer is somewhat larger than the one induced in the substrate layer: $0.040 \mu_B$ in 1Cu/1Co/Cu(001) and $0.035 \mu_B$ in 1Cu/2Co/Cu(001).

VI. ELECTRONIC PROPERTIES

The calculated electronic properties are consistent with the above discussed structural and energetic trends. Figure 3 shows the local density of states (LDOS) of the d -bands of the adsorbate and substrate layers obtained from a nonmagnetic calculation. For 1Co/Cu(001) the Co d -band is rather narrow, the LDOS at the Fermi level is very high and the overlap with the copper d -band is small, which reflects that the interaction between Co and Cu is not very strong. For the 2Co/Cu(001) system the d -states of the surface and subsurface Co layers overlap and their d -bands receive a substantial broadening. At the same time the LDOS at the Fermi level is lowered. The broadening of the cobalt d -bands in 2Co/Cu(001) is an indication for the strong interaction between the two cobalt layers. The same effect of broadening of the d -band of Co is observed for 1Cu/2Co/Cu(001) compared

to the Co d -band in 1Cu/1Co/Cu(001).

The layer-resolved LDOS of the d -bands for the ferromagnetic systems is given in Fig. 4. The majority band of Co is completely filled and the minority band is only partly filled, reflecting the fact that Co is a strong ferromagnet. For 1CoFM/Cu(001) and 1Cu/1CoFM/Cu(001) the Fermi level crosses the minority d -band of cobalt almost at its maximum while for 2CoFM/Cu(001) and 1Cu/2CoFM/Cu(001) the Fermi level lies in a dip of the Co d -bands. A “harder” electronic structure, i.e. lower density at the Fermi level is typically considered an indication for a more stable system.

Both majority and minority d -bands of copper are occupied and lie ca. 2 eV below the Fermi level. Still the minority and majority d -band have a very different structure with the majority band being broader in general. Actually the band width correlates with the strength of interaction with the cobalt film: While there is a substantial overlap between the majority d -bands of cobalt and the substrate layer beneath or the capping layer above, the corresponding minority bands have a very small overlap.

VII. COMPARISON OF CO/CU(001) AND CO/CU(111)

Prior to our work Pedersen *et al.*¹⁵ studied the growth of Co on the (111) surface of Cu with STM and LMTO-calculations. The STM measurements showed that the islands consist of several cobalt layers with the lowest layer possibly growing subsurface. At elevated temperatures vacancy islands formed in the terraces close to steps and the substrate material etched from these holes covered the cobalt islands.

Comparing the LMTO calculations for nonmagnetic systems with [111]-orientation¹⁵ with our FP-LAPW results for the [001]-orientation we note that the general behavior is similar: The systems are unstable against phase separation and clustering. The energy gain from the separation of a monolayer film in a bilayer island and a clean Cu surface is $\Delta E_{(001)} = 0.59 \text{ eV}/(1 \times 1)\text{-cell}$ and $\Delta E_{(111)} = 0.39 \text{ eV}/(1 \times 1)\text{-cell}$ respectively. The corresponding energy gain for the capped systems is $\Delta E_{(100)} = 0.31 \text{ eV}/(1 \times 1)\text{-cell}$ and $\Delta E_{(111)} = 0.18 \text{ eV}/(1 \times 1)\text{-cell}$.

The segregation of Cu onto the surface lowers the energy of the system for both orientations: for monolayer coverages $\Delta E_{(100)} = 0.49 \text{ eV}/(1 \times 1)\text{-cell}$ and $\Delta E_{(111)} = 0.30 \text{ eV}/(1 \times 1)\text{-cell}$; for 2ML of Co $\Delta E_{(100)} = 0.42 \text{ eV}/(1 \times 1)\text{-cell}$ and $\Delta E_{(111)} = 0.20 \text{ eV}/(1 \times 1)\text{-cell}$.

Still in all cases the energy gain is lower for the (111) surface than the (100) surface. This trend reflects the difference in coordination numbers: In a bond cutting model of metallic bonding the energy of an atom roughly scales as the square root of the local coordination^{41,34}.

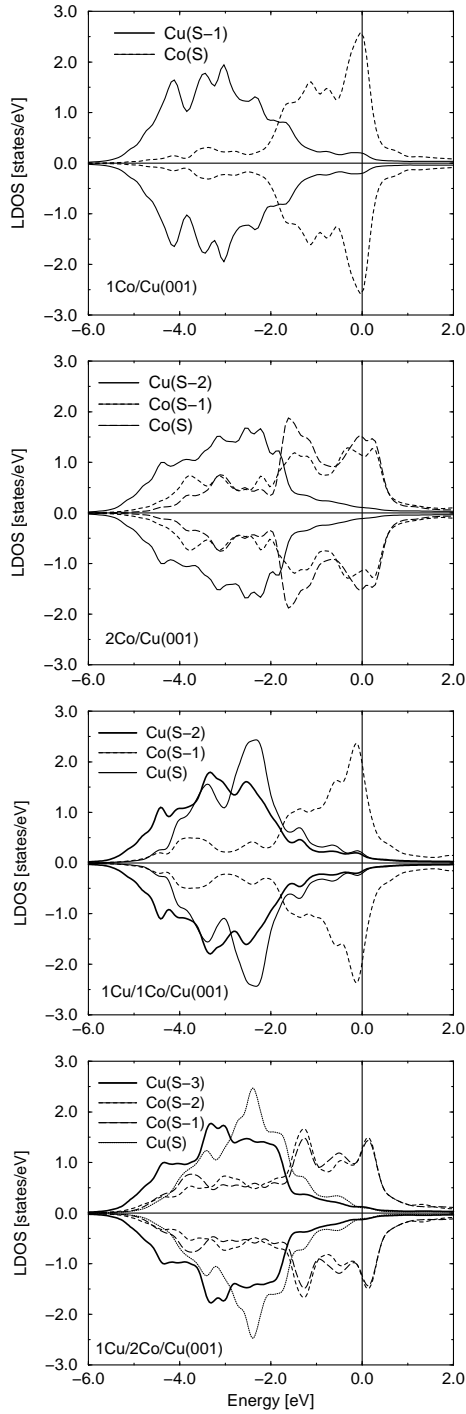


FIG. 3. Local density of states of the d -bands of the different atomic layers in the nonmagnetic systems. S, S-1, S-2, S-3 denote the surface and the subsequent subsurface layers respectively. We display the contribution from inside the muffin-tin spheres. The Co bands are represented with dashed and long-dashed lines, the Cu bands with a solid line. The calculated LDOS was broadened by a Gaussian with a width of $2\sigma = 0.2$ eV.

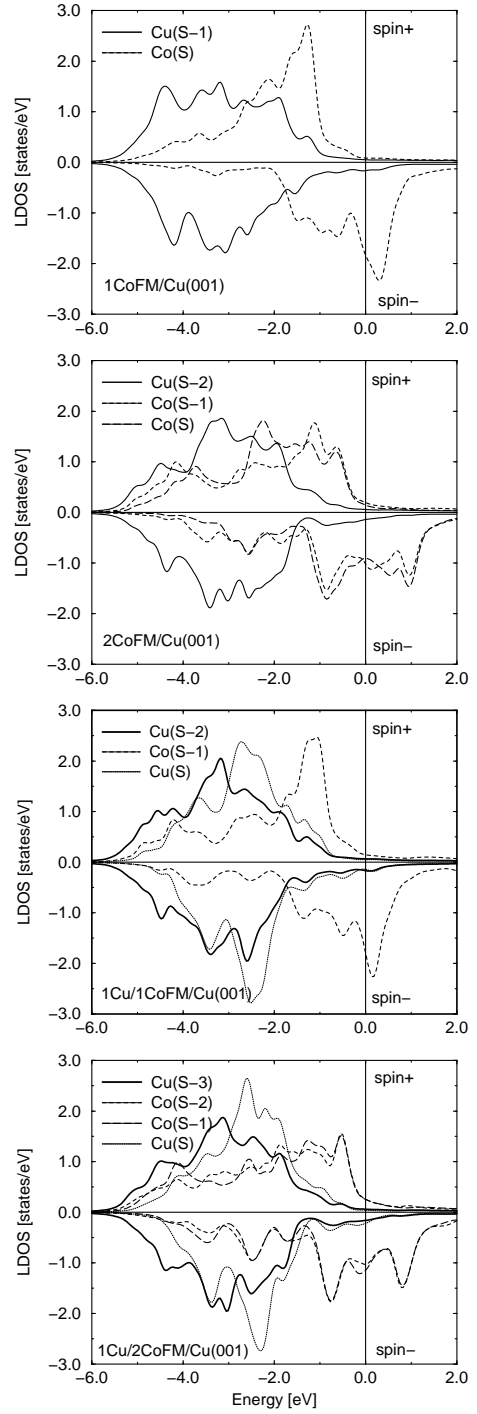


FIG. 4. LDOS of the d -bands of the different atomic layers in the ferromagnetic systems. S, S-1, S-2, S-3 denote the surface and the subsequent subsurface layers respectively. The contribution from inside the muffin-tin spheres is displayed. The Co bands are marked with dashed and long-dashed lines, the Cu bands with a solid line. The calculated LDOS was broadened by a Gaussian with a width of $2\sigma = 0.2$ eV.

Adsorption of a Co layer or of a Cu capping layer implies a change of coordination of the atoms in the added layer from 4 to 8 for the [100]- and from 6 to 9 for the [111]-orientation. And for the atoms in the layer, which after adsorption becomes the second layer, the coordination changes from 8 to 12 for the [100]- and from 9 to 12 for the [111]-orientation. Thus, the energy gain is smaller for the [111]-orientation than for the [100]-orientation.

VIII. SUMMARY

In summary, we identify a bilayer cobalt island covered by copper as the lowest energy configuration. However, growth is ruled by kinetics. Therefore, it is to be expected that under realistic conditions metastable structures may exist at surfaces, and some examples were identified in this paper. Total-energy considerations show that the (1×1) -film tends to separate into areas of bilayer cobalt islands and clean copper surface, and this is indeed in line with experimental observations of bilayer growth^{7,8,42}. Our total energy and electron density of states results show that the stability of the bilayer film is due to the fact that the Co atoms prefer to attain a high coordination of alike atoms. A consequence of this is the very strong contraction of the interlayer distance between the two cobalt layers and the substantial broadening of the cobalt d -bands in the adsorbed Co-bilayer as compared to the d -band of a single Co adlayer.

The segregation of substrate material onto the Co adlayer results in a substantial energy gain $0.5 \text{ eV}/(1 \times 1)$ -cell). We also studied a two-layer surface alloy of Co and Cu with a $c(2 \times 2)$ periodicity. This is found to be energetically less favorable than a separation into Cu-capped Co bilayer-adsorbates, but at strained regions of the surface this surface alloy may be stabilized. Indeed, a $c(2 \times 2)$ surface structure was observed in recent combined STM and RHEED experiments²⁹.

Generally, the ferromagnetically ordered systems are lower in energy than the nonmagnetic, but the relative stability of different configurations remains qualitatively unchanged by magnetism and the structural trends are well described by the nonmagnetic systems.

For low coverages ($\Theta < 0.25 \text{ ML}$) we also find that cobalt may adsorb substitutionally^{44,45}. However, with increasing coverage the substitutional adsorption becomes energetically unfavorable compared to the formation of compact islands.

ACKNOWLEDGMENTS

We gratefully acknowledge discussions with P. Kratzer, P. Ruggerone, and P. M. Marcus. We also thank M. Farle and K. Baberschke for stimulating discussions. The work was supported by the DFG through SFB290. We thank A. Chaka for a careful reading of the manuscript.

System	$E_{\text{LDA}}^{\text{f}}$	$E_{\text{GGA}}^{\text{f}}$
Cu(001)	0.78	0.61
1Co/Cu(001) NM	1.75	1.47
1Co/Cu(001) FM	1.54	1.22
2Co/Cu(001) NM	1.55	1.27
2Co/Cu(001) FM	1.48	1.11
1Cu/1Co/Cu(001) NM	1.26	0.99
1Cu/2Co/Cu(001) NM	1.13	0.85

TABLE VIII. The formation energies $E_{\text{LDA}}^{\text{f}}$ and $E_{\text{GGA}}^{\text{f}}$ of the different configurations calculated within LDA and GGA, respectively, given in [$\text{eV}/(1 \times 1)$ -cell]. The lateral parameter is set to the corresponding (LDA or GGA) equilibrium lattice constant of copper.

IX. APPENDIX

For several systems we performed calculations with the LDA¹⁶ and with the GGA¹⁷. The formation energies for 1Co/Cu(001) (NM and FM), 2Co/Cu(001) (NM and FM), 1Cu/1Co/Cu(001), and 1Cu/2Co/Cu(001) are given in Table VIII. The lateral parameter was set to the lattice constants of copper obtained within the LDA and GGA approach, respectively. The LDA value 3.55 \AA is 1.7% smaller than the measured one, 3.61 \AA , while with the GGA the lattice parameter (3.65 \AA) is 1.1% bigger than the experimental value (zero-point vibrations are neglected in the theory).

The formation energies obtained with the GGA are generally lower than the LDA results and the differences are between 0.2 and 0.3 $\text{eV}/(1 \times 1)$ -cell. This effect was also observed previously for the clean copper surface⁴³. Yet the trends between the different configurations remain unchanged. For example the energy gain from the separation of a monolayer cobalt film in a bilayer cobalt island and clean Cu(001)-surface is $0.60 \text{ eV}/(1 \times 1)$ -cell (LDA) and $0.53 \text{ eV}/(1 \times 1)$ -cell (GGA) for the nonmagnetic systems and $0.41 \text{ eV}/(1 \times 1)$ -cell (LDA) and $0.36 \text{ eV}/(1 \times 1)$ -cell (GGA) for the ferromagnetically ordered systems. The equilibrium configuration of clean copper surface with bilayer cobalt islands, covered by copper (see Fig. 1(f)), is by $0.79 \text{ eV}/(1 \times 1)$ -cell (LDA) and by $0.74 \text{ eV}/(1 \times 1)$ -cell (GGA) more favorable than 1Co/Cu(001) in Fig. 1(a).

A structural optimization was performed for all systems listed in Table VIII using both approaches, LDA and GGA. No noticeable differences were obtained except for the systems, containing a bilayer cobalt film, where the contraction of the distance between the two cobalt layers was slightly stronger with the GGA, e.g. for 2Co/Cu(001) $\Delta d_{\text{Co-Co}}^{\text{LDA}}/d_0^{\text{LDA}} = 17\%$ and $\Delta d_{\text{Co-Co}}^{\text{GGA}}/d_0^{\text{GGA}} = 18.6\%$. However, these minor differences do not alter the discussion in Section IV.

The larger lateral parameter in GGA produces a substantial enhancement of the magnetic moments, e.g. the surface magnetic moment of cobalt in 1Co/Cu(001) changes from $1.71 \mu_B$ (LSDA) to $1.86 \mu_B$ (GGA) and in

2Co/Cu(001) from $M_{\text{Co(S)}}^{\text{LSDA}} = 1.71 \mu_B$ and $M_{\text{Co(S-1)}}^{\text{LSDA}} = 1.47 \mu_B$ to $M_{\text{Co(S)}}^{\text{GGA}} = 1.81 \mu_B$ and $M_{\text{Co(S-1)}}^{\text{GGA}} = 1.64 \mu_B$. This result is not surprising and is in line with the changes of the magnetic moment for fcc cobalt bulk from $1.52 \mu_B$ (LSDA) to $1.69 \mu_B$ (GGA).

In conclusion, both approximations of the exchange-correlation potential, LDA and GGA, lead to the same results for the structural, energetic, and magnetic properties of the configurations studied in this work.

-
- ¹ G. Binasch, P. Grünberg, F. Saurenbach, and W. Zinn, Phys. Rev. B **39**, 4828 (1989).
- ² P. Bruno, Phys. Rev. B **52**, 411 (1995).
- ³ P. Bruno and C. Chappert, Phys. Rev. Lett. **67**, 1602 (1991).
- ⁴ P. Alippi, P. M. Marcus, and M. Scheffler, Phys. Rev. Lett. **78**, 3892 (1997).
- ⁵ R. Pentcheva and S. Blügel, to be published; Jülich Reports **3364** (1997).
- ⁶ J. Fassbender, R. Allenspach, and U. Dürig, Surf. Sci. **383**, L 742 (1997).
- ⁷ H. Li and B. P. Tonner, Surf. Sci. **237**, 141 (1990).
- ⁸ J. R. Cerda, P. L. de Andres, A. Cebollada, R. Miranda, E. Navas, P. Schuster, C. M. Schneider, and J. Kirschner, J. Phys.: Cond. Matt **5**, 2055 (1993).
- ⁹ A. K. Schmid, A. Atlan, H. Itoh, B. Heinrich, T. Ichinokawa, and J. Kirschner, Phys. Rev. B **48**, 2855 (1993).
- ¹⁰ J. Shen, J. Giergel, A. K. Schmid, and J. Kirschner, Surf. Sci. **328**, 32 (1995).
- ¹¹ U. Bovensiepen, P. Pouloupoulos, W. Platow, M. Farle, and K. Baberschke, J. Magn. Magn. Mat. **192**, L386 (1999).
- ¹² R. Wu and A. J. Freeman, J. Appl. Phys. **79**, 6500 (1996).
- ¹³ S. Blügel, *Habilitationsschrift*, RWTH Aachen, (1995).
- ¹⁴ O. Erikson, A. M. Boring, R. C. Albers, G. W. Fernando, and B. R. Cooper, Phys. Rev. B **45**, 2868 (1992).
- ¹⁵ M. Ø. Pedersen, I. A. Bönicke, E. Lægsgaard, I. Stensgaard, A. Ruban, J. K. Nørskov, and F. Besenbacher, Surf. Sci. **387**, 86, (1997).
- ¹⁶ J. P. Perdew and Y. Wang, Phys. Rev. B **45**, 13244 (1992).
- ¹⁷ J.P. Perdew, S. Burke, and M. Ernzerhof, Phys. Rev. Lett. **77**, 3865, (1996).
- ¹⁸ P. Blaha, K. Schwarz and J. Luitz, WIEN97, A Full Potential Linearized Augmented Plane Wave Package for Calculating Crystal Properties, (Karlheinz Schwarz, Techn. Univ. Wien, Vienna 1999). ISBN 3-9501031-0-4 Updated version of P. Blaha, K. Schwarz, P. Sorantin, and S. B. Trickey, Comp. Phys. Commun. **59**, 399, 1990.
- ¹⁹ M. Petersen, F. Wagner, L. Hufnagel, and M. Scheffler, accepted for publication in Comp. Phys. Commun.
- ²⁰ B. Kohler, S. Wilke, M. Scheffler, R. Kouba and C. Ambrosch-Draxl, Comp. Phys. Commun. **94**, 31 (1996).
- ²¹ The area of a (1×1) -structure is 6.30 \AA^2 .
- ²² H. J. Monkhorst and J. D. Pack, Phys. Rev. B **18**, 45897 (1978).
- ²³ Q. T. Jiang, P. Fenter, and T. Gustafsson, Phys. Rev. B **44**, 5773 (1991).
- ²⁴ H. L. Davis and J. R. Noonan, Surf. Sci. **126**, 245 (1983).
- ²⁵ P. O. Gartland, S. Berge, and B. J. Slagsvold, Phys. Rev. Lett. **28**, 738 (1973).
- ²⁶ G. A. Haas and R. E. Thomas, J. Appl. Phys. **48**, 86 (1977).
- ²⁷ G. G. Tibbets, J. M. Burkstrand, and J. C. Tracy, Phys. Rev. B **15**, 3652 (1977).
- ²⁸ A. Saúl and M. Weissmann, Phys. Rev. B **60**, 4982 (1999).
- ²⁹ F. Nouvertné, U. May, A. Rampe, M. Gruyters, U. Korte, R. Berndt, and G. Güntherodt, Surf. Sci. Letters, in print.
- ³⁰ The calculations for bilayer $c(2 \times 2)$ -alloy were performed with the same cutoff parameters as for the (1×1) -structures (see Section II and 15 \mathbf{k}_{\parallel} -points in the irreducible wedge of the Brillouin-zone.
- ³¹ B. Poelsema, private communication.
- ³² For fct cobalt with $a_{\parallel} = a_{\text{Cu}}$ we obtained the following distances in z -direction: $a_z^{\text{NM}} = 3.23 \text{ \AA}$ and $a_z^{\text{FM}} = 3.31 \text{ \AA}$.
- ³³ We note here that the formation energy of Co(001) was also calculated with respect to fct cobalt bulk in order to separate the elastic from the electronic effects.
- ³⁴ M. Methfessel, D. Henning, and M. Scheffler, Appl. Phys. A **55**, 442 (1992).
- ³⁵ The fact that the equilibrium lattice constant of a free-standing Co monolayer is noticeably smaller than the lattice constant of Co (or Cu) bulk reflects that the low coordination of atoms in the free-standing monolayer leads to a stronger bonding between the cobalt atoms and thus shorter bond lengths. This result follows Pauling's description of the relation between coordination, bond strength, and bond length.
- ³⁶ A. Clarke, G. Jennigs, R. F. Willis, P. J. Rous, and J. B. Pendry, Surf. Sci. **187**, 327 (1987).
- ³⁷ M. Farle *et al.*, priv. communication.
- ³⁸ P. Srivastava, F. Wilhelm, A. Ney, M. Farle, H. Wende, N. Haack, G. Ceballos, and K. Baberschke, Phys. Rev. B **58**, 5701 (1998).
- ³⁹ W. Clemens, T. Kachel, O. Rader, E. Vescovo, S. Blügel, C. Carbone, and W. Eberhardt, Solid State Commun. **81**, 739 (1992).
- ⁴⁰ M. Methfessel, D. Henning, and M. Scheffler, Phys. Rev. B **46**, 4816 (1992).
- ⁴¹ D. Spanjaard and Desjonquères in *Interaction of Atoms and Molecules with Solid Surfaces*, ed. by V. Bortolani (Plenum, New York, 1990).
- ⁴² A. K. Schmid, and J. Kirschner, Ultramicroscopy **4-44**, 483 (1992).
- ⁴³ G. Boisvert and L. J. Lewis, Phys. Rev. B **56**, 7643 (1997).
- ⁴⁴ F. Nouvertné, U. May, M. Bammig, A. Rampe, U. Korte, G. Güntherodt, R. Pentcheva and M. Scheffler, Phys. Rev. B, in print.
- ⁴⁵ R. Pentcheva and M. Scheffler, to be submitted.